Photocurrent spectroscopy of InAs/GaAs self-assembled quantum dots

P. W. Fry,[1] I. E. Itskevich,[2] S. R. Parnell,[1] J. J. Finley,[1] L. R. Wilson,[1] K. L. Schumacher,[1] D. J. Mowbray,[1] M. S. Skolnick,[1] M. Al-Khafaji,[3] A. G. Cullis,[3] M. Hopkinson,[3] J. C. Clark,[3] and G. Hill[3]

[1]*Department of Physics and Astronomy, University of Sheffield, S3 7RH, United Kingdom*

[2]*Institute for Solid-State Physics, Russian Academy of Sciences, Chernogolovka, Moscow district, 142432, Russia*

[3]*Department of Electronic and Electrical Engineering, University of Sheffield, S1 3JD, United Kingdom*

(Received 21 April 2000)

Photocurrent (PC) spectroscopy is employed to study several important aspects of the interband optoelectronic properties of InAs/GaAs self-assembled quantum dots (SAQDs). PC spectroscopy is first shown to be a highly sensitive, quantitative technique to measure the interband absorption spectra of SAQDs. Up to four well-defined features are observed in the spectra arising from transitions between confined hole and electron levels. The transition energies are shown to agree well with those observed in electroluminescence, with negligible Stokes shifts found, contrary to previous reports. Large quantum-confined Stark shifts of the transitions are observed in PC spectroscopy as discussed in detail elsewhere [Fry *et al.* Phys. Rev. Lett. **84**, 733, (2000)]. Discrete interband transitions are observed superimposed on a broad background signal, shown to arise in part from field-dependent transitions into tail states of the two-dimensional wetting layer and the GaAs cladding region. A field-independent contribution to the background is also found, possibly from dots with larger size and shape fluctuations than those which give rise to the resolved interband transitions. By comparison of photocurrent signals from quantum dots and the wetting layer within the same sample, it is demonstrated that the quantum-dot oscillator strength is not significantly modified relative to that of a quantum well of the same surface area, consistent with performance found from quantum-dot laser devices. Polarization studies for in-plane light propagation are reported. The measurements show that the observed interband transitions involve predominantly heavy-hole-like levels, consistent with an assumption of theoretical modelling of Stark-effect results. Finally carrier escape mechanisms from the dots are deduced, with tunneling found to dominate at low temperature, and thermally activated escape becoming increasingly important at temperatures above ~100 K. Carrier escape is shown to occur from a common level, the ground state, demonstrating that excited-state to ground-state relaxation is faster than direct excited-state escape.

I. INTRODUCTION

In recent years InAs/GaAs self-assembled quantum dots have been the subject of intense interest as a result of their discrete, zero-dimensional electronic states,[1] their excellent optoelectronic quality, and their favorable characteristics for applications such as ultralow threshold lasers[1] and memory devices.[2] Despite this, many questions regarding their electronic properties remain unanswered, due in part to the limitations inherent in many of the spectroscopic techniques employed to date. In particular, absorption measurements which provide fundamental information (energies, oscillator strengths, polarizations, selection rules, etc.) on interband optical transitions, and which are directly comparable to theoretical predictions, have been very difficult to perform. To a large degree this is because the fractional absorption by a single layer of dots is very small ($\sim 10^{-4}-10^{-5}$). Since the structural characteristics of successive layers dots are likely to differ,[3] this difficulty is not easily overcome by growing multiple-dot layers, as employed routinely to measure quantum-well absorption spectra.[4] Furthermore, photoluminescence-excitation spectroscopy, which has been used extensively to measure the properties of higher-dimensional systems,[5] does not reproduce absorption spectra directly, but instead reflects intradot relaxation features associated with the emission of multiple LO phonons.[6,7] The only reports of absorption spectra have been from direct transmission measurements which required the use of extremely sensitive techniques with integration times of several hours per scan,[8] and from the very low-temperature technique of calorimetric absorption spectroscopy, which appeared to yield broadened spectra.[9]

In this work we demonstrate that photocurrent (PC) spectroscopy is a direct, sensitive, and relatively simple technique to measure low-noise absorption spectra of quantum dots.[10] The experiments are carried out in *p-i-n* (or *n-i-p*) diode structures, which permit electric fields up to $\sim 3 \times 10^5$ V/cm to be applied to the dots. We have shown elsewhere that such studies allow the observation of strong quantum-confined Stark effects, permitting detailed structural information on the dots to be deduced.[11] Here we show that studies as a function of electric field and temperature are able to reveal the relative importance of different carrier escape mechanisms from the dots, enable polarized light spectroscopy to be performed, and permit the origin of the quantization, giving rise to the excited-state transitions to be deduced. The quantum-dot (QD) spectra exhibit up to four features which are attributed to interband transitions between confined electron and hole states. The interband features are observed superimposed on a broad background spectrum, arising in part from band-tail absorption from the GaAs cladding/InAs wetting layer. We note that short-circuit PC measurements on InAs dots were reported recently by Chu *et al.*[12] using an in-plane light propagation geometry. Quali-

0163-1829/2000/62(24)/16784(8)/$15.00 PRB 62 16 784 ©2000 The American Physical Society

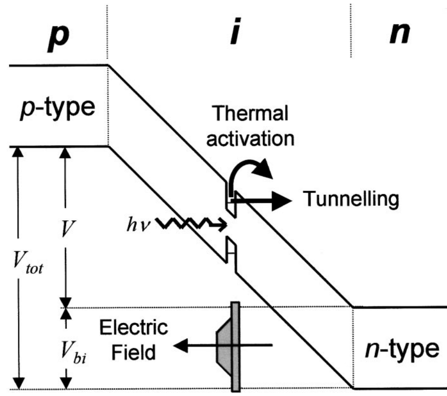

FIG. 1. Schematic band diagram under reverse bias of a *p-i-n* junction sample containing a single layer of quantum dots. An interband absorption process is indicated, followed by carrier escape either by tunneling or by thermal excitation, thus leading to the observed photocurrent signals. The strongly truncated quantum dot shape employed in Ref. 11 to fit the observed Stark shift data is shown. The electric-field direction indicated corresponds to reverse bias.

tatively similar, but significantly less well-resolved spectra to those reported here were obtained.

The paper is organised in the following way. In Sec. II details of the samples and of the experimental techniques are described. This is followed in Sec. III A by the presentation of normal-incidence photocurrent spectra for several different samples, from which it is shown that absorption spectra of the dots are measured and that absolute values for the absorption strengths can be deduced. In Sec. III B the electric-field dependence of the interband transitions and of a broad underlying background is presented for samples with and without dots. In Sec. III C, polarized spectra for in-plane propagation are presented, and in Sec. III D we deduce carrier escape mechanisms from the dots. Finally in Sec. IV we summarize the main conclusions.

II. EXPERIMENT

All samples were fabricated using solid-source molecular beam epitaxy on GaAs(001) substrates. Both *p-i-n* (p^+ region uppermost) and *n-i-p* (n^+ region uppermost) were studied. For *p-i-n* structures 250-nm n^+-GaAs regions were first grown on n^+ substrates followed by a 300–550-nm undoped GaAs intrinsic region. 2.4-ML-thick InAs quantum-dot layers, grown by Stranski-Krastanow techniques at a temperature of 500 °C, were embedded in the center of the intrinsic region. The intrinsic region was capped by a 300-nm-thick p^+-GaAs contact layer. To enable electrical contact, circular annular contact mesas of diameter 400 μm were defined, and the samples mounted and bonded on standard transistor headers. Reverse biasing results in an electric field of up to 3×10^5 V/cm oriented along the growth axis from substrate to surface. *n-i-p* structures were fabricated on semi-insulating GaAs substrates by reversing the doping sequence in the buffer layer and the contact layers, thus enabling electric fields to be applied in the opposite direction to that of the *p-i-n* structures.

The band profile for a typical *p-i-n* device is illustrated in Fig. 1. For reverse applied bias, large electric fields could be

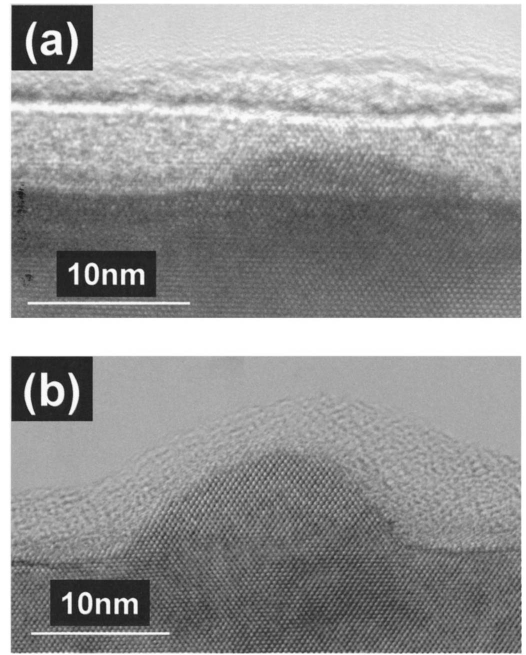

FIG. 2. Cross-sectional transmission electron micrographs of uncapped fast (a) and slow (b) growth rate quantum dots. The dots used for the photocurrent spectroscopy are capped by 1500- or 2500-Å GaAs.

applied in the intrinsic region with negligible dark current (<1 nA) through the device up to ~10 V. Capacitance-voltage measurements carried out on the structures showed that the width of the intrinsic region width (W_i) remained constant, equal to within 10% to the nominal growth width, across the entire bias range studied. As a result it can be concluded that all the applied bias was dropped across the intrinsic region, and that the electric field (F) in the intrinsic region is given by

$$F=(V_A+V_{bi})/W_i, \tag{1}$$

where V_A is the applied reverse bias and V_{bi} is the built-in potential of the diode (~1.5 V).

Quantum dots grown under two distinct sets of growth conditions were investigated. The first type was grown at ~0.09 ML/s, leading to lens-shaped quantum dots of ~3-nm height and ~15-nm base length, as evidenced from cross-sectional transmission electron microscopy (TEM) as shown in Fig. 2(a). From plan-view TEM the areal density was found to be $9.6\times10^{10}\,\mathrm{cm}^{-2}$. For the second dot type the InAs was deposited at the slower rate of 0.01 ML/s. This produced taller dots with an approximate height of 6 nm (base ~18 nm), as shown in Fig. 2(b), and a lower areal dot density of $3.5\times10^{10}\,\mathrm{cm}^{-2}$.

The structural parameters of the samples studied are summarized in Table I. Samples 2 and 3 were designed as laser structures, and contain additional 1.5-μm-thick $Al_{0.6}Ga_{0.4}As$ cladding layers either side of the GaAs intrinsic region. For the growth of the cladding layers the growth temperature was increased to ~650 °C, resulting in some annealing of the dots and a shift of their interband transitions to ~100 meV higher energy. Additionally, sample 3 contains five layers of quantum dots separated by GaAs spacer layers of thickness 25 nm.

TABLE I.

Sample number	Device type	Total intrinsic width W_i (nm)	InAs deposition rate (ML/s)	No. of dot layers/spacer width (nm)
1	*p-i-n*	500	0.09	1
2	*n-i-p*	525	0.087	1
3	*n-i-p*	550	0.087	5/25
4	*p-i-n*	300	0.01	1
5	*p-i-n*	300	0.01	1
6	*n-i-p*	300	0.01	1
7	*p-i-n*	300	0.09	Wetting layer only
8	*p-i-n*	220	0.01	1

Photocurrent spectra were investigated using ac lock-in techniques at ~100 Hz, with the samples illuminated for most of the measurements in normal-incidence geometry by monochromated white light from a tungsten halogen lamp. Low-intensity illumination of ~3 mW cm^{-2} was employed, corresponding to dot occupancies $\ll 1$, where the spectra are unperturbed by many carrier occupation effects.

III. RESULTS AND DISCUSSION

A. General aspects of photocurrent spectra and comparison with electroluminescence

In this section we present PC spectra at zero applied bias for several representative samples, and investigate how the spectra depend on factors such as areal density and number of dot layers. In Fig. 3(a), we show PC spectra for samples $S1$ (fast growth) and $S4$ ($S4$ slow growth) at a temperature of 300 K. The spectra consist of three ($S1$) or four ($S4$) features arising from interband transitions in the QD's, superimposed on a broad background signal which strongly increases in intensity to higher energy. As indicated schematically in Fig. 1, electron-hole pairs created by interband absorption escape from the dots and give rise to the measured photocurrent. The carrier escape mechanisms are analyzed in detail in Sec. III D. However, for the moment, the important point is that for zero applied bias at temperatures >200 K (the present experimental conditions) all carriers created by interband absorption escape from the dots and contribute to the photocurrent. As a result it is expected that the PC spectra provide a quantitative representation of the absorption spectra of the QD's.

The expectation is supported by the results in Figs. 3(a) and 3(b). In Fig. 3(a) the magnitude of the PC signal for the fast growth dots ($S1$) is found to be ~3 times greater than for the slow growth dots ($S4$), consistent with the ~3 times higher density of these dots. In Fig. 3(b), we compare spectra from samples $S2$ and $S3$, fast growth dots containing one- and five-dot layers respectively. The five-dot sample was grown with spacer layers of 25 nm, thus ensuring that there is no electronic coupling between the successive dot layers. The PC spectra of the two samples are very similar in overall form to those in Fig. 3(a), with a series of interband transitions again observed. Most importantly the intensities of the transitions in $S3$ are, to a very good approximation, a factor

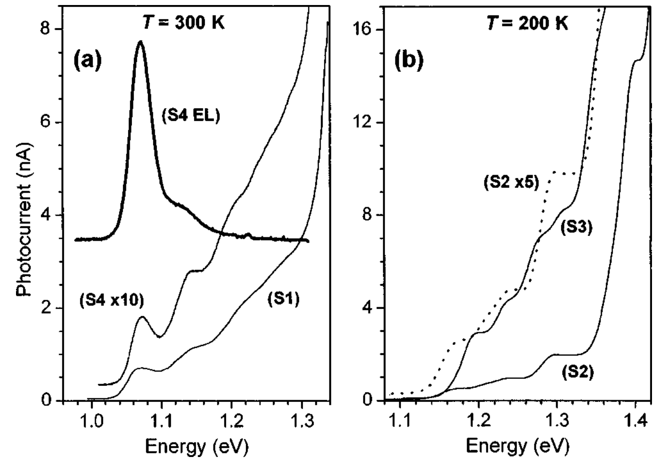

FIG. 3. (a) Photocurrent spectra at 300 K and zero applied bias for samples $S1$ (slow growth) and $S4$ (fast growth), showing 3 ($S1$) and four ($S4$) interband transitions. The ground-state photocurrent signal from the fast-growth-rate dots is a factor of 3 stronger than for the low-growth-rate dots, consistent with the ~3 times higher density in these samples. Interband transitions are observed, superimposed on a broad background PC signal, strongly increasing to higher energy. A low current electroluminescence spectrum from sample $S4$ is also shown in the upper part of the figure. The energies of the ground-state transitions are seen to agree well in EL and PC. (b) Comparison of single-layer ($S2$) and five-layer ($S3$) dot samples. The five-layer sample is seen to exhibit ~5 times the PC intensity of the single-layer sample.

of 5 stronger than those in $S2$, as seen from the close similarity in intensity between the $S3$ spectrum and the dotted curve corresponding to the $S2$ spectrum multiplied by a factor of 5. The results in Figs. 3(a) and 3(b) thus both demonstrate that the PC signals are directly proportional to the number of quantum dots in the samples, and thus suggest strongly that true absorption spectra are being measured.

Prior to the present work, nearly all interband spectra for InAs dots were obtained by emission (luminescence) spectroscopy, and have formed the basis for nearly all theoretical modeling of the electronic states. It is thus important to compare the PC spectra with emission spectra, and to determine, for example, whether the observed transition energies are the same. Such a comparison is shown in Fig. 3(a) where 300 K low-current electroluminescence (EL) spectra[13] for sample $S4$ are compared with the PC from the same sample. Very good agreement between the ground state transition energies in PC and EL is found, providing further support to the interpretation of the PC as arising from interband transitions in the dots. There has been another comparison of PC and EL published recently by Chu *et al.*[12] These authors found (Stokes) shifts between EL and PC of ~10–15 meV. This behavior is possibly due to the larger linewidths in their samples, leading to the possibility of selective carrier escape from smaller dots in PC, resulting in a shift of the PC peak to higher energy than in EL.

As well as permitting the form of the absorption spectra of the QD's to be deduced, PC spectroscopy also enables absolute values for the absorption strength (A) of the QD transitions to be deduced. Under conditions where all the photocreated carriers escape from the QD's, and hence con-

tribute to the PC signal, the magnitude of the photocurrent signal I is related to the total incident optical power P at frequency v by

$$I = APe/hv. \quad (2)$$

To determine I for the ground-state transition a (small) linear background subtraction was performed to account for the background contribution (see Sec. III B) to the photocurrent. P was measured using a calibrated optical power meter, and corrected for reflection losses at the cryostat windows and at the air-semiconductor interface at the surface of the sample. Using this procedure we obtain peak values of A for ground-state transitions of $(2.8 \pm 0.3) \times 10^{-4}$ for sample 1 and $(8.7 \pm 1.2) \times 10^{-5}$ for sample 4. These values are in good agreement with that reported by Warburton *et al.* from direct transmission spectroscopy,[8] after taking into account the different areal dot densities. As noted in Sec. I, the measurements of Ref. 8 required very long measurement times and a highly stable experimental system. By comparison, the absorption spectra measured by PC are obtained by very straightforward experimental techniques in typical measurement scans of 5–10 min. The main reason for the high sensitivity of the PC techniques is that PC, unlike direct absorption, is a zero background technique, and furthermore currents can very easily be measured with sub pA sensitivity (single-dot-layer photocurrents under our experimental conditions are ~100 pA). In Sec. II B, quantitative comparison between the absorption strengths of dots and wetting layers in the same sample are made.

B. Electric-field dependence of spectra and broad background photocurrent

A series of spectra for sample $S5$ as a function of applied bias from 0 to 6 V (electric fields from 50 to 250 kV/cm) at a temperature of 200 K are shown in Fig. 4. A strong shift of the interband transitions to lower energy is observed due to the quantum confined Stark effect (see the inset to Fig. 4). The Stark shift results were discussed in detail elsewhere;[11,14] the analysis is not repeated here. The main conclusions reached were that the dots have a permanent dipole moment, with a sign opposite to that predicted by all accurate theoretical modeling. By comparison with modeling of the strain distribution and electronic structure calculations, it was shown that this result could only be explained if the dots had a severely truncated shape (see the schematic shape on Fig 1), and if the dots contained significant amounts of gallium graded from base to apex. The best fit to the Stark shift data for samples $S5$ and $S6$ is shown by the full line in the inset to Fig. 4.

It is notable that at all biases the QD interband transitions are superimposed on a broad background photocurrent signal, as noted in Sec. III A, whose intensity increases strongly with increasing photon energy. Spectra for sample $S4$ over a wide spectral range, presented in Fig. 5, show that the broad background signal extends up to and beyond the photocurrent peak arising from transitions into the two-dimensional wetting layer at 1.36 eV. It is also notable in Figs. 4 and 5 that the strength of the background signal in the 1.2–1.3-eV range increases markedly with increasing field applied to the sample.

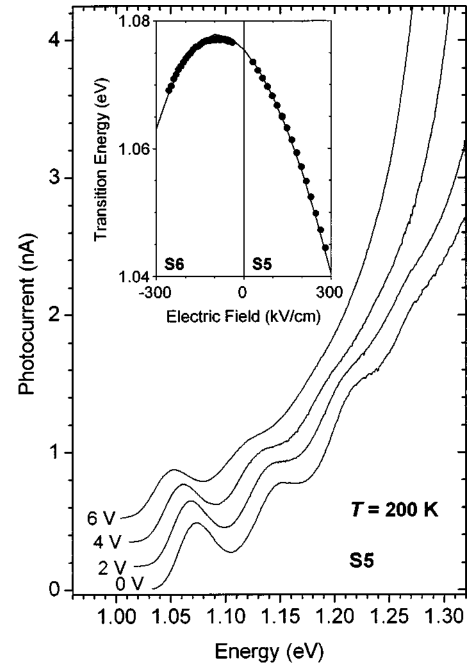

FIG. 4. Photocurrent spectra for sample $S5$ as a function of applied bias at a temperature of 200 K. A strong Stark shift to lower energy of the interband transitions is seen. At higher energy the background signal underlying the interband transitions is seen to increase markedly in intensity with increasing bias, and to shift to lower energy. The inset shows the ground-state transition energies for the consecutively grown *p-i-n* and *n-i-p* samples (samples $S5$ and $S6$) as a function of electric field, together with a fit to the theoretical model of Refs. 11 and 14.

To investigate the origin of the background signal, an additional sample, $S7$, containing only the wetting layer but no quantum dots was investigated. This was achieved by depositing 1.5 ML of InAs during growth, before the transition from two- to three-dimensional growth occurred. When studied in photoluminescence (or electroluminescence), this sample showed only a wetting layer signal, with no characteristic quantum dot features observable.

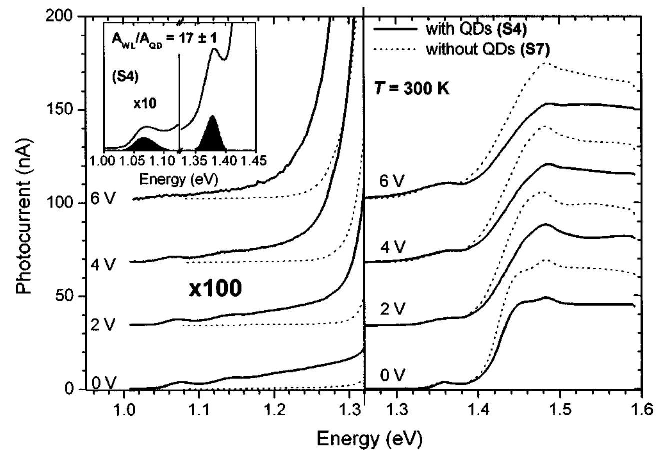

FIG. 5. Photocurrent spectra for samples $S4$ (quantum dots plus wetting layer) and $S7$ (wetting layer only) from 1 to 1.35 eV (a) and 1.3 to 1.6 eV (b) at 300 K. The inset shows PC spectra for the dots and wetting layer for sample $S4$. Spectra after subtraction of the respective backgrounds are shown shaded.

300-K PC spectra from this sample are shown in Fig. 5 together with the $S4$ spectra for direct comparison, for biases from 0 to 6 V. In the higher-energy range from 1.3 to 1.7 eV the spectra from the two samples are very similar, with clear peaks from the wetting layer and from the GaAs cladding being seen. From 1 to 1.3 eV the spectra from the two samples are very different, as expected, with the well-defined QD interband transitions being seen for sample $S4$ only. We now consider the bias dependence of the spectra. For both samples, the GaAs and wetting-layer (WL) signals are observed to broaden markedly with bias, most likely due to Franz-Keldysh effects in the high electric fields applied (250 kV/cm at 6 V).[15] As a result of this field-induced broadening, an increasingly strong tail of the WL/GaAs signals spreads down into the dot region (1.1–1.3 eV) as greater reverse bias is applied, clearly seen in Fig. 5. This tail gives rise to the increasingly strong PC signal with bias above 1.2 eV in Figs. 4 and 5. However, it is also clear from Fig. 5 that the WL/GaAs band-edge tail does not account for the broad background underlying the lower-energy interband transitions (below 1.2 eV), whose strength remains essentially field independent up to the highest biases applied. The origin of the background underlying the lower-energy interband transitions thus remains unclear at the present time. A possible explanation for this is that it arises from dots with large size fluctuation which do not contribute to the well-resolved PC transitions, but instead contribute a broad background signal. An alternative speculative interpretation is that mixing between the discrete dot levels and the surrounding electronic continuum gives rise to a smoothly varying background underlying the discrete states.

It is interesting to note that a similar background signal was reported in direct transmission measurements by Warburton *et al.*[8] and by Chu *et al.* in PC,[12] and that a contribution from a continuous distribution of states to PL excitation spectra of single dots was reported by Toda *et al.*,[16] suggesting that such features are a general characteristic of dot absorption spectra. It is also notable that such a prominent background signal is not observed in emission (either EL or photoluminescence) [see, e.g., Fig. 3(a)]. This suggests that carriers in these states have a low radiative efficiency, perhaps due to rapid relaxation to lower-energy states.[12]

Finally, in this subsection we directly compare the absorption strengths for the dots and the wetting layer in the same sample. Since the two types of signals both arise on significant background signals (particularly the wetting layer), we first carried out a background subtraction, performed by a linear interpolation of the background feature between the high-and low-energy regions of the particular signals, and then subtraction from the observed spectra. The results are shown in the inset of Fig. 5. A ratio of the integrated intensities of dots to a wetting layer of 0.06 (17^{-1}) is found. Within experimental errors this value is close to the areal coverage of the dots in sample $S4$ of 0.1. It can thus be concluded that within experimental error there is no significant modification of the oscillator strength for optical absorption in the dots compared to the wetting layer, in agreement with recent theoretical analysis,[17] and as expected for dots with a lateral size on the order of the exciton Bohr radius. This conclusion is also in agreement with analysis of the modal gain in quantum-dot lasers (QDL's) and comparison with that in quantum-well lasers (QWL's), where it is found that modal gains in QDL's relative to QWL's scale approximately with the areal coverage of the dots.[18]

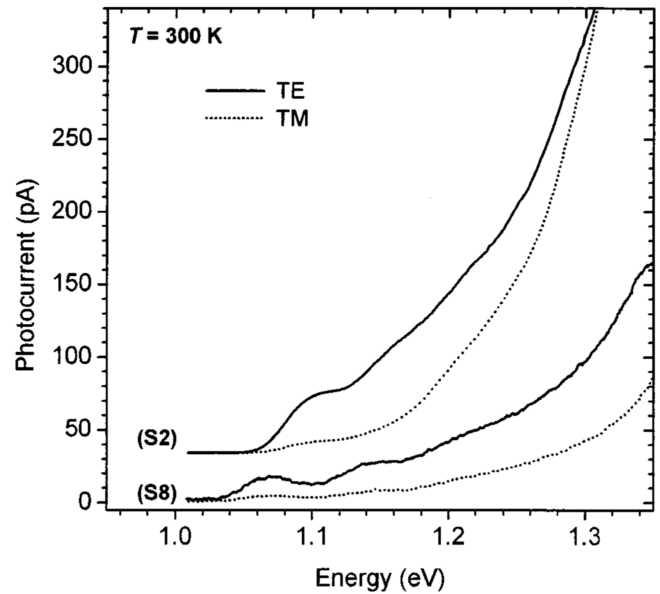

FIG. 6. Polarization-dependent spectra for in-plane propagation for samples $S2$ and $S8$ The spectra are observed to be strongly TE polarized (electric vector in the plane of the layers), as expected for transitions involving predominantly heavy-hole-like valence-band states.

Similar quantum-dot wetting-layer comparisons were also carried out for low-growth-rate samples, with a ratio of integrated areas of 0.014 being found. This value is a factor of 3.5 less than found for the fast-growth-sample above, consistent with the factor of 3 lower dot density and the three-times-smaller dot photocurrent for the slow-growth samples discussed in Sec. III A; the dot-wetting-layer comparisons thus provide further support for the reliability of photocurrent techniques for quantitative analysis of quantum-dot absorption strengths.

C. Polarization-dependent spectra

In Sec. III A we showed that PC represents a direct means to measure the absorption spectra of QD's, and discussed the application of PC techniques to investigate the effects of applied electric fields on QD spectra. We now show that PC can be used to investigate polarization-dependent properties of QD's for light propagating in the growth plane of the layers.

The results were obtained on samples $S2$ and $S8$, samples grown with $Al_{0.6}Ga_{0.4}As$ cladding layers, required to achieve efficient in-plane light guiding. For these measurements and those in Sec. III D below, the light exiting the spectrometer was passed through a linear polarizer, and then into a polarization rotator, which permitted light of any desired polarization direction to be incident on the sample. Spectra are presented in Fig. 6 for light focused through a microscope objective on to a cleaved edge of the sample for both TE (electric vector in the plane of the QD's) and TM (electric vector parallel to the growth direction) polarizations. For both samples the spectra are observed to be strongly TE polarized (especially for sample $S8$, where the TE spectra are a

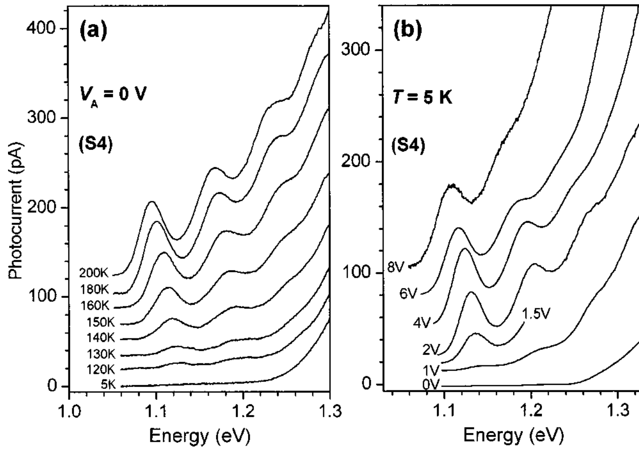

FIG. 7. (a) Zero-bias photocurrent spectra for sample $S4$ for temperatures from 5 to 200 K. At a low bias of 0 V and for temperatures less than ~100 K, only very weak photocurrent signals are observed from the interband QD transitions. For higher temperatures all the interband transitions show the same strongly thermally activated behavior, indicating carrier escape from a common level. (b) Photocurrent spectra for sample $S4$ at 5 K as a function of reverse bias. The interband QD transitions only have significant strength for reverse biases in excess of ~1.5 V, showing the dominance of tunneling escape at low temperature.

factor of 6 stronger). As mentioned briefly in Ref. 11, and also in Ref. 12, this shows that the lowest energy states are predominantly heavy hole in character,[19] an important assumption of the theoretical modelling of Refs. 11 and 14.

Polarization-dependent studies were also carried in the normal-incidence geometry of the previous sections. However, no measurable in-plane polarization anisotropy between the [110], [010], and [−110] directions ([001] growth direction) was found within our experimental accuracy of 5%.

D. Carrier escape mechanisms

We now turn our attention to an analysis of the carrier escape mechanisms in quantum dots. As noted in Sec. III A and indicated schematically in Fig. 1, electron-hole pairs created by the interband absorption escape from the quantum dots are swept to the contacts, and give rise to the observed photocurrent. In order to understand the nature of the escape mechanisms, photocurrent spectra were recorded over a wide range of temperature and electric field.

Figure 7(a) displays a series of spectra from sample 4 under zero applied bias (an electric field of 50 kV/cm) for temperatures from 5 to 200 K. At 5 K there are no observable interband features arising from the quantum dots, a weak signal being observed only at energies >1.25 eV, from band-tail absorption of the wetting layer and GaAs cladding regions, as discussed previously. Under these conditions, carriers created by optical absorption into QD's cannot escape, and instead undergo radiative recombination. As the temperature is raised to ~120 K, well-defined but weak features appear in the spectrum. In the range 130–200 K the peaks become increasingly more intense with increasing temperature, reflecting the rising probability for carrier escape as the thermal energy increases; for these low applied fields, carrier escape from the dots by thermal activation is thus only significant for temperatures $\gtrsim 120$ K. For temperatures above 200 K, no further change in the magnitude of the photocurrent is observed, showing that under conditions of zero applied bias all photoexcited carriers escape from the dots and contribute to the photocurrent, and thus that the PC provides a true representation of the absorption spectra of the dots.

It is notable that the PC spectra for ground and excited-state transitions all show the same temperature dependence. This indicates that following interband excitation, thermally activated escape always occurs from the same confined energy levels (the electron-hole ground states), and thus that the relaxation rate from excited to ground states ($\sim 3 \times 10^{11}\,\mathrm{sec}^{-1}$) (Ref. 20) is faster than any competing thermal or tunneling escape rates.

The conclusion that the excited- to ground-state relaxation is faster than any excited-state tunneling rate provides evidence for the origin of the quantization, which gives rise to the excited to ground-state energy splittings, and for the nature of the excited-state wave functions. The electron and hole ground-state wave functions are expected to have no nodes in both vertical and lateral directions, with the dominant energy upshift arising from quantization in the (small) vertical direction.[21] The observation that the relaxation rate from excited to ground states is faster than any excited-state tunneling rates shows that excited states must have approximately the same vertical extent as the ground state, and hence that the excited-state–ground-state splittings must arise from predominantly lateral quantization. If, instead, the excited-state wave functions were more extended in the vertical (z) direction than the ground state (i.e., were the second confined levels in the z direction), tunnel escape from these levels would be expected to dominate. Using Wentzel-Kramers-Brillouin (WKB) methods, we estimate very rapid tunneling rates of $>10^{12}\,\mathrm{sec}^{-1}$ for a z-like excited state of an ionization energy of 50 meV even for electric fields of less than 50 kV/cm,[22] very much faster than the relaxation rate of $\sim 3\times 10^{11}\,\mathrm{sec}^{-1}$. This conclusion regarding the lateral quantization origin of the excited states is consistent with that obtained in Ref. 11 from the observation of identical Stark shifts for all the QD interband transitions.

In Fig. 7(b), spectra are presented as a function of bias (V_A), at a low temperature of 5 K where there is no escape by thermal excitation. As in Fig. 7(a) ($T<100$ K) at low bias (<0.5 V, electric field <65 kV/cm), only the band-tail signal from the wetting layer/GaAs interface is observed. With increasing bias, the well-defined interband transitions become increasingly prominent, and reach their full intensity for biases greater than 3 V (fields > 150 kV/cm) when all carriers escape from the dots. This behavior is consistent with tunneling being the dominant carrier escape mechanism from the dots at low temperature, with carrier escape again occurring from a common level (the ground state),[23] since all the interband transitions show the same bias dependence (as discussed above for the temperature-dependent behavior). Similar to the discussion of the temperature-dependent data above, this result shows that excited-state–ground-state splittings arise predominantly from lateral quantization, since if

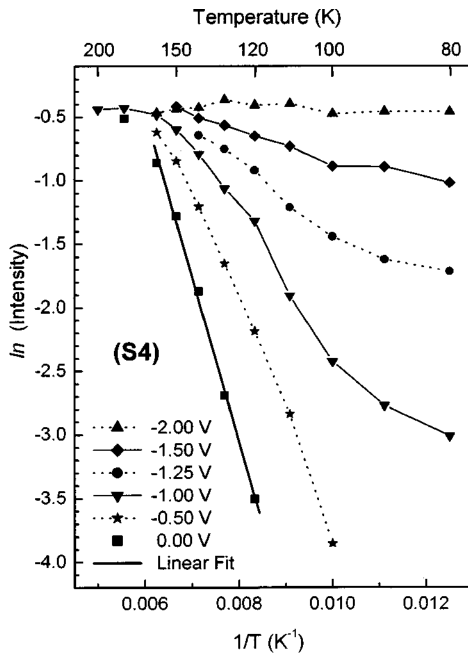

FIG. 8. Arrhenius plots of ground-state photocurrent intensities for sample $S4$ at reverse biases from 0 to 2 V. From the slope of the 0-V results, where thermal escape dominates, an activation energy of 130 meV is deduced. With increasing bias the slopes of the (nonexponential) Arrhenius plots decrease as tunneling becomes increasingly important, until at 2 V the escape becomes temperature independent.

the excited-state wave functions were more extended along the growth direction (i.e., were due to additional vertical quantization), tunneling from these states would be very rapid and the transitions starting from high-energy would appear successively with increasing bias, contrary to experiment.

The interband PC signals are expected to reach their full intensity with increasing field when the tunneling time of the carriers which can tunnel most rapidly from the dots becomes less than the radiative recombination time ($\sim$1 ns).[24] WKB estimates of tunneling times show that for a field of $\sim$50 kV/cm, when tunneling is first observed, ground-state tunneling times are expected to be in the range 1–10 nsec for electrons, and many orders of magnitude greater for heavy holes due to the $>$5 times higher hole mass.[25,26] Such estimates (probably only accurate to within an order of magnitude) are well known to be highly sensitive to input parameters (carrier masses, band offsets, etc.). They nevertheless are consistent with the conclusion that the photocurrent signal becomes observable at low temperature when electron tunneling from the wells occurs. The small decrease of the features with bias for $V_A > 3$ V is due to field-induced reduction of the transition oscillator strength as the electron-hole overlap decreases in high field, as discussed in Ref. 11.

The results of Figs. 7(a) and 7(b) are presented more quantitatively in Fig. 8 on an Arrhenius plot of ground-state transition intensities against $1/T$, for biases between 0 and 2 V. At low bias (0 V) a reasonable straight-line behavior is found on the Arrhenius plots, in the regime where thermal activation was concluded above to be the dominant escape mechanism. For biases $\geqslant$0.5 V, the Arrhenius plots become increasingly nonlinear with decreasing average slopes, until at 2 V the temperature dependence is very small as tunneling becomes the dominant escape mechanism. A thermal activation energy of 95 ± 20 meV is obtained from the slope of the 0-V data. This value is significantly less than the estimated energy separations (ΔE_s) between the dot ground electron and hole levels and their respective band edges of $\sim$200 meV.[21,27] The agreement with theory is improved somewhat if comparison is made with the energy separation from dot ground state to wetting layer when the calculated excitation energies are reduced by about 30 meV (Ref. 27) to $\sim$170 meV, closer to the experimental values particularly when one allows for the possibility of band tail conduction in the wetting layer (see Sec. III B), and for possible uncertainties in the theoretical values for ΔE_s. It is also worth pointing out that our experimental value is in very good agreement with that found in the deep-level transient spectroscopy experiments of Kapteyn *et al.*[28] where an electron thermal activation energy of 95 meV was reported from n-type devices containing QD's with similar photoluminescence emission energies to those in the present work, the authors invoking a two-step excitation process to explain the rather low observed activation energy.

IV. CONCLUSIONS

Photocurrent spectroscopy has been shown to be a direct, versatile, and precise experimental technique for measuring absorption spectra of quantum dots. Comparison of spectra from samples grown under differing growth conditions, and with differing numbers of dot layers in the samples, have established that true absorption spectra are measured at temperatures $\geqslant$200 K. The dot transitions are observed to be superimposed on a broad background signal whose intensity increases strongly to higher photon energy. By comparison with spectra from a sample containing only the wetting layer and no dots, the broad background has been shown to arise in part from field-dependent transitions into tail states of the wetting layer or of the GaAs barriers, as well as a field-independent part of less certain origin. The field-independent part is suggested to arise either from a broad background distribution of dots, or perhaps from mixing between the discrete dot levels and continuum states of the surrounding GaAs. For light propagating in the plane of the samples, the transitions have been shown to be predominantly in-plane polarized, consistent with a major assumption of theoretical Stark effect modeling. Finally, it has been shown that carrier escape from the dots occurs from a common level, the dot ground state, showing that the relaxation rate from excited to ground states is faster than escape by either tunneling or thermal activation.

ACKNOWLEDGMENTS

We wish to thank J. A. Barker and E. P. O'Reilly for invaluable discussions on the theory of the electronic structure of quantum dots. We also acknowledge financial support from EPSRC, Grant No. GR/L28821, RFBR, GNTP, and DERA.

[1] D. Bimberg, M. Grundmann, and N. N. Ledenstov, *Quantum Dot Heterostructures* (Wiley, New York, 1998).
[2] J. J. Finley, M. Skalitz, M. Arzberger, A. Zrenner, G. Böhm, and G. Abstreiter, Appl. Phys. Lett. **73**, 2618 (1998).
[3] See, e.g., N. N. Ledentsov, M. Grundmann, N. Kirstaedter, O. Schmidt, R. Heitz, J. Bohrer, D. Bimberg, V. M. Ustinov, V. A. Shchukin, A. Y. Egorov, A. E. Zhukov, S. Zaitsev, P. S. Kop'ev, Zh. I. Alferov, S. S. Ruvimov, A. O. Kosogov, P. Werner, U. Gosele, and J. Heydenreich, Solid State Electron. **40**, 785 (1996).
[4] See, e.g., R. Dingle, W. Wiegmann, and C. H. Henry, Phys. Rev. Lett. **33**, 827 (1974).
[5] C. Weisbuch, R. Dingle, A. C. Gossard, and W. Wiegmann, Solid State Commun. **38**, 709 (1981).
[6] M. J. Steer, D. J. Mowbray, W. R. Tribe, M. S. Skolnick, M. D. Sturge, M. Hopkinson, A. G. Cullis, C. R. Whitehouse, and R. Murray, Phys. Rev. B **54**, 17 738 (1996).
[7] R. Heitz, M. Grundmann, N. N. Ledenstov, L. Eckey, M. Veit, D. Bimberg, V. M. Ustinov, A. Yu. Egorov, A. E. Zhukov, P. S. Kop'ev, and Zh. I. Alferov, Appl. Phys. Lett. **68**, 361 (1996).
[8] R. J. Warburton, C. S. Durr, K. Karrai, J. P. Kotthaus, G. Medeiros-Ribeiro, and P. M. Petroff, Phys. Rev. Lett. **79**, 5282 (1997).
[9] M. Grundmann *et al.*, Phys. Rev. Lett. **74**, 4043 (1995).
[10] The power of photocurrent spectroscopy for measuring the absorption spectra of quantum wells was pointed out by R. T. Collins, K. v. Klitzing, and K. Ploog, Phys. Rev. B **33**, 4378 (1986).
[11] P. W. Fry, I. E. Itskevich, D. J. Mowbray, M. S. Skolnick, J. J. Finley, J. A. Barker, E. P. O'Reilly, L. R. Wilson, I. A. Larkin, P. A. Maksym, M. Hopkinson, M. Al-Khafaji, J. P. R. David, A. G. Cullis, G. Hill, and J. C. Clark, Phys. Rev. Lett. **84**, 733 (2000).
[12] L. Chu, M. Arzberger, A. Zrenner, G. Bohm, and G. Abstreiter, Appl. Phys. Lett. **75**, 2247 (1999); A further observation of a large Stokes shift has recently been reported. See A. Patenè, A. Levin, A. Polimeni, L. Eaves, P. C. Main, and M. Henini, Phys. Rev. B **62**, 11 084 (2000).
[13] At low current the EL spectra are unperturbed by many carrier occupation effects, and are thus directly comparable to the PC spectra.
[14] J. A. Barker and E. P. O'Reilly, Phys. Rev. B **61**, 13 840 (2000).
[15] See *Semiconductors and Semimetals*, edited by R. K. Willardson and A. C. Beer (Academic Press, 1972), Chaps. 1 and 6.
[16] Y. Toda, O. Moriwaki, M. Nishioka, and Y. Arakawa, Phys. Rev. Lett. **82**, 4114 (1999).
[17] L. C. Andreani, G. Panzarini, and J. M. Gerard, Phys. Rev. B **60**, 13 276 (1999).
[18] P. W. Fry, L. Harris, S. R. Parnell, J. J. Finley, A. D. Ashmore, D. J. Mowbray, M. S. Skolnick, M. Hopkinson, G. Hill, and J. C. Clark, J. Appl. Phys. **87**, 615 (2000).
[19] G. Bastard, *Wave Mechanics Applied to Semiconductor Heterostructures* (Wiley, New York, 1988), p. 248.
[20] R. Heitz, M. Veit, N. N. Ledenstov, A. Hoffmann, D. Bimberg, V. M. Ustinov, P. S. Kop'ev, and Zh. I. Alferov, Phys. Rev. B **56**, 10 435 (1997).
[21] See e.g., O. Stier, M. Grundmann, and D. Bimberg, Phys. Rev. B **59**, 5688 (1999).
[22] For this estimate we approximated the dot by a 50-Å-wide potential well, assumed an electron mass of $0.6m_e$, and took the energy separation (ΔE_s) between the excited state and the continuum to be 50 meV. At an electric field of 50 kV/cm, tunneling times are at least three orders of magnitude greater for the ground state, with, e.g., ΔE_s of 200 meV.
[23] As for the discussion of the temperature-dependent data, this result shows that excited states arise from lateral quantization, since, if their wave functions have one or more nodes in the growth direction i.e., are due to vertical quantization, tunneling from these states will be very rapid and transitions starting from high energy will appear successively with increasing bias, contrary to experiment.
[24] P. D. Buckle, P. Dawson, S. A. Hall, X. Chen, M. J. Steer, D. J. Mowbray, M. S. Skolnick, and M. Hopkinson, J. Appl. Phys. **86**, 2555 (1999).
[25] As for the excited-state estimate in Ref. 22, tunneling times were calculated for a 50-Å InAs quantum well in GaAs barriers, assuming a 60:40 split in the offset between the conduction and valence bands, with $m_e=0.06m_e$, $m_{hh}=0.4m_e$, an electron ground-state ionization energy of 200 meV, and a hole ground-state ionization energy of 200 meV.
[26] Similar conclusions regarding the respective electron and hole tunneling times were reached in Ref. 2, and in M. C. Bodefeld, R. J. Warburton, K. Karrai, J. P. Kotthaus, G. Medeiros-Ribeiro, and P. M. Petroff, Appl. Phys. Lett. **74**, 1839 (1999).
[27] L. W. Wang, A. J. Williamson, A. Zunger, H. Jiang, and J. Singh, Appl. Phys. Lett. **76**, 339 (2000).
[28] C. M. A. Kapteyn, F. Heinrichsdorff, O. Stier, R. Heitz, M. Grundmann, N. D. Zakharov, D. Bimberg, and F. Werner, Phys. Rev. B **60**, 14 265 (1999).